BABAR-CONF-10/003
SLAC-PUB-14210

Evidence for $B^+ \to \tau^+ \nu_\tau$ decays using hadronic B tags

P. del Amo Sanchez,[1] J. P. Lees,[1] V. Poireau,[1] E. Prencipe,[1] V. Tisserand,[1] J. Garra Tico,[2] E. Grauges,[2] M. Martinelli[ab],[3] D. A. Milanes,[3] A. Palano[ab],[3] M. Pappagallo[ab],[3] G. Eigen,[4] B. Stugu,[4] L. Sun,[4] D. N. Brown,[5] L. T. Kerth,[5] Yu. G. Kolomensky,[5] G. Lynch,[5] I. L. Osipenkov,[5] H. Koch,[6] T. Schroeder,[6] D. J. Asgeirsson,[7] C. Hearty,[7] T. S. Mattison,[7] J. A. McKenna,[7] A. Khan,[8] A. Randle-Conde,[8] V. E. Blinov,[9] A. R. Buzykaev,[9] V. P. Druzhinin,[9] V. B. Golubev,[9] E. A. Kravchenko,[9] A. P. Onuchin,[9] S. I. Serednyakov,[9] Yu. I. Skovpen,[9] E. P. Solodov,[9] K. Yu. Todyshev,[9] A. N. Yushkov,[9] M. Bondioli,[10] S. Curry,[10] D. Kirkby,[10] A. J. Lankford,[10] M. Mandelkern,[10] E. C. Martin,[10] D. P. Stoker,[10] H. Atmacan,[11] J. W. Gary,[11] F. Liu,[11] O. Long,[11] G. M. Vitug,[11] C. Campagnari,[12] T. M. Hong,[12] D. Kovalskyi,[12] J. D. Richman,[12] A. M. Eisner,[13] C. A. Heusch,[13] J. Kroseberg,[13] W. S. Lockman,[13] A. J. Martinez,[13] T. Schalk,[13] B. A. Schumm,[13] A. Seiden,[13] L. O. Winstrom,[13] C. H. Cheng,[14] D. A. Doll,[14] B. Echenard,[14] D. G. Hitlin,[14] P. Ongmongkolkul,[14] F. C. Porter,[14] A. Y. Rakitin,[14] R. Andreassen,[15] M. S. Dubrovin,[15] G. Mancinelli,[15] B. T. Meadows,[15] M. D. Sokoloff,[15] P. C. Bloom,[16] W. T. Ford,[16] A. Gaz,[16] M. Nagel,[16] U. Nauenberg,[16] J. G. Smith,[16] S. R. Wagner,[16] R. Ayad,[17,*] W. H. Toki,[17] H. Jasper,[18] T. M. Karbach,[18] A. Petzold,[18] B. Spaan,[18] M. J. Kobel,[19] K. R. Schubert,[19] R. Schwierz,[19] D. Bernard,[20] M. Verderi,[20] P. J. Clark,[21] S. Playfer,[21] J. E. Watson,[21] M. Andreotti[ab],[22] D. Bettoni[a],[22] C. Bozzi[a],[22] R. Calabrese[ab],[22] A. Cecchi[ab],[22] G. Cibinetto[ab],[22] E. Fioravanti[ab],[22] P. Franchini[ab],[22] E. Luppi[ab],[22] M. Munerato[ab],[22] M. Negrini[ab],[22] A. Petrella[ab],[22] L. Piemontese[a],[22] R. Baldini-Ferroli,[23] A. Calcaterra,[23] R. de Sangro,[23] G. Finocchiaro,[23] M. Nicolaci,[23] S. Pacetti,[23] P. Patteri,[23] I. M. Peruzzi,[23,†] M. Piccolo,[23] M. Rama,[23] A. Zallo,[23] R. Contri[ab],[24] E. Guido[ab],[24] M. Lo Vetere[ab],[24] M. R. Monge[ab],[24] S. Passaggio[a],[24] C. Patrignani[ab],[24] E. Robutti[a],[24] S. Tosi[ab],[24] B. Bhuyan,[25] V. Prasad,[25] C. L. Lee,[26] M. Morii,[26] A. Adametz,[27] J. Marks,[27] U. Uwer,[27] F. U. Bernlochner,[28] M. Ebert,[28] H. M. Lacker,[28] T. Lueck,[28] A. Volk,[28] P. D. Dauncey,[29] M. Tibbetts,[29] P. K. Behera,[30] U. Mallik,[30] C. Chen,[31] J. Cochran,[31] H. B. Crawley,[31] L. Dong,[31] W. T. Meyer,[31] S. Prell,[31] E. I. Rosenberg,[31] A. E. Rubin,[31] A. V. Gritsan,[32] Z. J. Guo,[32] N. Arnaud,[33] M. Davier,[33] D. Derkach,[33] J. Firmino da Costa,[33] G. Grosdidier,[33] F. Le Diberder,[33] A. M. Lutz,[33] B. Malaescu,[33] A. Perez,[33] P. Roudeau,[33] M. H. Schune,[33] J. Serrano,[33] V. Sordini,[33,‡] A. Stocchi,[33] L. Wang,[33] G. Wormser,[33] D. J. Lange,[34] D. M. Wright,[34] I. Bingham,[35] C. A. Chavez,[35] J. P. Coleman,[35] J. R. Fry,[35] E. Gabathuler,[35] R. Gamet,[35] D. E. Hutchcroft,[35] D. J. Payne,[35] C. Touramanis,[35] A. J. Bevan,[36] F. Di Lodovico,[36] R. Sacco,[36] M. Sigamani,[36] G. Cowan,[37] S. Paramesvaran,[37] A. C. Wren,[37] D. N. Brown,[38] C. L. Davis,[38] A. G. Denig,[39] M. Fritsch,[39] W. Gradl,[39] A. Hafner,[39] K. E. Alwyn,[40] D. Bailey,[40] R. J. Barlow,[40] G. Jackson,[40] G. D. Lafferty,[40] T. J. West,[40] J. Anderson,[41] R. Cenci,[41] A. Jawahery,[41] D. A. Roberts,[41] G. Simi,[41] J. M. Tuggle,[41] C. Dallapiccola,[42] E. Salvati,[42] R. Cowan,[43] D. Dujmic,[43] G. Sciolla,[43] M. Zhao,[43] D. Lindemann,[44] P. M. Patel,[44] S. H. Robertson,[44] M. Schram,[44] P. Biassoni[ab],[45] A. Lazzaro[ab],[45] V. Lombardo[a],[45] F. Palombo[ab],[45] S. Stracka[ab],[45] L. Cremaldi,[46] R. Godang,[46,§] R. Kroeger,[46] P. Sonnek,[46] D. J. Summers,[46] X. Nguyen,[47] M. Simard,[47] P. Taras,[47] G. De Nardo[ab],[48] D. Monorchio[ab],[48] G. Onorato[ab],[48] C. Sciacca[ab],[48] G. Raven,[49] H. L. Snoek,[49] C. P. Jessop,[50] K. J. Knoepfel,[50] J. M. LoSecco,[50] W. F. Wang,[50] L. A. Corwin,[51] K. Honscheid,[51] R. Kass,[51] J. P. Morris,[51] N. L. Blount,[52] J. Brau,[52] R. Frey,[52] O. Igonkina,[52] J. A. Kolb,[52] R. Rahmat,[52] N. B. Sinev,[52] D. Strom,[52] J. Strube,[52] E. Torrence,[52] G. Castelli[ab],[53] E. Feltresi[ab],[53] N. Gagliardi[ab],[53] M. Margoni[ab],[53] M. Morandin[a],[53] M. Posocco[a],[53] M. Rotondo[a],[53] F. Simonetto[ab],[53] R. Stroili[ab],[53] E. Ben-Haim,[54] G. R. Bonneaud,[54] H. Briand,[54] G. Calderini,[54] J. Chauveau,[54] O. Hamon,[54] Ph. Leruste,[54] G. Marchiori,[54] J. Ocariz,[54] J. Prendki,[54] S. Sitt,[54] M. Biasini[ab],[55] E. Manoni[ab],[55] A. Rossi[ab],[55] C. Angelini[ab],[56] G. Batignani[ab],[56] S. Bettarini[ab],[56] M. Carpinelli[ab],[56,¶] G. Casarosa[ab],[56] A. Cervelli[ab],[56] F. Forti[ab],[56] M. A. Giorgi[ab],[56] A. Lusiani[ac],[56] N. Neri[ab],[56] E. Paoloni[ab],[56] G. Rizzo[ab],[56] J. J. Walsh[a],[56] D. Lopes Pegna,[57] C. Lu,[57] J. Olsen,[57] A. J. S. Smith,[57] A. V. Telnov,[57] F. Anulli[a],[58] E. Baracchini[ab],[58] G. Cavoto[a],[58] R. Faccini[ab],[58] F. Ferrarotto[a],[58] F. Ferroni[ab],[58] M. Gaspero[ab],[58] L. Li Gioi[a],[58] M. A. Mazzoni[a],[58] G. Piredda[a],[58] F. Renga[ab],[58] T. Hartmann,[59] T. Leddig,[59] H. Schröder,[59] R. Waldi,[59] T. Adye,[60] B. Franek,[60] E. O. Olaiya,[60] F. F. Wilson,[60] S. Emery,[61] G. Hamel de Monchenault,[61] G. Vasseur,[61] Ch. Yèche,[61] M. Zito,[61] M. T. Allen,[62] D. Aston,[62] D. J. Bard,[62] R. Bartoldus,[62] J. F. Benitez,[62] C. Cartaro,[62] M. R. Convery,[62] J. Dorfan,[62] G. P. Dubois-Felsmann,[62] W. Dunwoodie,[62] R. C. Field,[62] M. Franco Sevilla,[62] B. G. Fulsom,[62] A. M. Gabareen,[62] M. T. Graham,[62] P. Grenier,[62] C. Hast,[62] W. R. Innes,[62] M. H. Kelsey,[62]

Work supported in part by US Department of Energy contract DE-AC02-76SF00515.

SLAC National Accelerator Laboratory, Menlo Park, CA 94025

H. Kim,[62] P. Kim,[62] M. L. Kocian,[62] D. W. G. S. Leith,[62] S. Li,[62] B. Lindquist,[62] S. Luitz,[62] V. Luth,[62] H. L. Lynch,[62] D. B. MacFarlane,[62] H. Marsiske,[62] D. R. Muller,[62] H. Neal,[62] S. Nelson,[62] C. P. O'Grady,[62] I. Ofte,[62] M. Perl,[62] T. Pulliam,[62] B. N. Ratcliff,[62] A. Roodman,[62] A. A. Salnikov,[62] V. Santoro,[62] R. H. Schindler,[62] J. Schwiening,[62] A. Snyder,[62] D. Su,[62] M. K. Sullivan,[62] S. Sun,[62] K. Suzuki,[62] J. M. Thompson,[62] J. Va'vra,[62] A. P. Wagner,[62] M. Weaver,[62] W. J. Wisniewski,[62] M. Wittgen,[62] D. H. Wright,[62] H. W. Wulsin,[62] A. K. Yarritu,[62] C. C. Young,[62] V. Ziegler,[62] X. R. Chen,[63] W. Park,[63] M. V. Purohit,[63] R. M. White,[63] J. R. Wilson,[63] S. J. Sekula,[64] M. Bellis,[65] P. R. Burchat,[65] A. J. Edwards,[65] T. S. Miyashita,[65] S. Ahmed,[66] M. S. Alam,[66] J. A. Ernst,[66] B. Pan,[66] M. A. Saeed,[66] S. B. Zain,[66] N. Guttman,[67] A. Soffer,[67] P. Lund,[68] S. M. Spanier,[68] R. Eckmann,[69] J. L. Ritchie,[69] A. M. Ruland,[69] C. J. Schilling,[69] R. F. Schwitters,[69] B. C. Wray,[69] J. M. Izen,[70] X. C. Lou,[70] F. Bianchi[ab],[71] D. Gamba[ab],[71] M. Pelliccioni[ab],[71] M. Bomben[ab],[72] L. Lanceri[ab],[72] L. Vitale[ab],[72] N. Lopez-March,[73] F. Martinez-Vidal,[73] A. Oyanguren,[73] J. Albert,[74] Sw. Banerjee,[74] H. H. F. Choi,[74] K. Hamano,[74] G. J. King,[74] R. Kowalewski,[74] M. J. Lewczuk,[74] C. Lindsay,[74] I. M. Nugent,[74] J. M. Roney,[74] R. J. Sobie,[74] T. J. Gershon,[75] P. F. Harrison,[75] T. E. Latham,[75] E. M. T. Puccio,[75] H. R. Band,[76] S. Dasu,[76] K. T. Flood,[76] Y. Pan,[76] R. Prepost,[76] C. O. Vuosalo,[76] and S. L. Wu[76]

(The *BABAR* Collaboration)

[1]*Laboratoire d'Annecy-le-Vieux de Physique des Particules (LAPP), Université de Savoie, CNRS/IN2P3, F-74941 Annecy-Le-Vieux, France*
[2]*Universitat de Barcelona, Facultat de Fisica, Departament ECM, E-08028 Barcelona, Spain*
[3]*INFN Sezione di Bari[a]; Dipartimento di Fisica, Università di Bari[b], I-70126 Bari, Italy*
[4]*University of Bergen, Institute of Physics, N-5007 Bergen, Norway*
[5]*Lawrence Berkeley National Laboratory and University of California, Berkeley, California 94720, USA*
[6]*Ruhr Universität Bochum, Institut für Experimentalphysik 1, D-44780 Bochum, Germany*
[7]*University of British Columbia, Vancouver, British Columbia, Canada V6T 1Z1*
[8]*Brunel University, Uxbridge, Middlesex UB8 3PH, United Kingdom*
[9]*Budker Institute of Nuclear Physics, Novosibirsk 630090, Russia*
[10]*University of California at Irvine, Irvine, California 92697, USA*
[11]*University of California at Riverside, Riverside, California 92521, USA*
[12]*University of California at Santa Barbara, Santa Barbara, California 93106, USA*
[13]*University of California at Santa Cruz, Institute for Particle Physics, Santa Cruz, California 95064, USA*
[14]*California Institute of Technology, Pasadena, California 91125, USA*
[15]*University of Cincinnati, Cincinnati, Ohio 45221, USA*
[16]*University of Colorado, Boulder, Colorado 80309, USA*
[17]*Colorado State University, Fort Collins, Colorado 80523, USA*
[18]*Technische Universität Dortmund, Fakultät Physik, D-44221 Dortmund, Germany*
[19]*Technische Universität Dresden, Institut für Kern- und Teilchenphysik, D-01062 Dresden, Germany*
[20]*Laboratoire Leprince-Ringuet, CNRS/IN2P3, Ecole Polytechnique, F-91128 Palaiseau, France*
[21]*University of Edinburgh, Edinburgh EH9 3JZ, United Kingdom*
[22]*INFN Sezione di Ferrara[a]; Dipartimento di Fisica, Università di Ferrara[b], I-44100 Ferrara, Italy*
[23]*INFN Laboratori Nazionali di Frascati, I-00044 Frascati, Italy*
[24]*INFN Sezione di Genova[a]; Dipartimento di Fisica, Università di Genova[b], I-16146 Genova, Italy*
[25]*Indian Institute of Technology Guwahati, Guwahati, Assam, 781 039, India*
[26]*Harvard University, Cambridge, Massachusetts 02138, USA*
[27]*Universität Heidelberg, Physikalisches Institut, Philosophenweg 12, D-69120 Heidelberg, Germany*
[28]*Humboldt-Universität zu Berlin, Institut für Physik, Newtonstr. 15, D-12489 Berlin, Germany*
[29]*Imperial College London, London, SW7 2AZ, United Kingdom*
[30]*University of Iowa, Iowa City, Iowa 52242, USA*
[31]*Iowa State University, Ames, Iowa 50011-3160, USA*
[32]*Johns Hopkins University, Baltimore, Maryland 21218, USA*
[33]*Laboratoire de l'Accélérateur Linéaire, IN2P3/CNRS et Université Paris-Sud 11, Centre Scientifique d'Orsay, B. P. 34, F-91898 Orsay Cedex, France*
[34]*Lawrence Livermore National Laboratory, Livermore, California 94550, USA*
[35]*University of Liverpool, Liverpool L69 7ZE, United Kingdom*
[36]*Queen Mary, University of London, London, E1 4NS, United Kingdom*
[37]*University of London, Royal Holloway and Bedford New College, Egham, Surrey TW20 0EX, United Kingdom*
[38]*University of Louisville, Louisville, Kentucky 40292, USA*
[39]*Johannes Gutenberg-Universität Mainz, Institut für Kernphysik, D-55099 Mainz, Germany*
[40]*University of Manchester, Manchester M13 9PL, United Kingdom*
[41]*University of Maryland, College Park, Maryland 20742, USA*
[42]*University of Massachusetts, Amherst, Massachusetts 01003, USA*
[43]*Massachusetts Institute of Technology, Laboratory for Nuclear Science, Cambridge, Massachusetts 02139, USA*

[44]McGill University, Montréal, Québec, Canada H3A 2T8
[45]INFN Sezione di Milano[a]; Dipartimento di Fisica, Università di Milano[b], I-20133 Milano, Italy
[46]University of Mississippi, University, Mississippi 38677, USA
[47]Université de Montréal, Physique des Particules, Montréal, Québec, Canada H3C 3J7
[48]INFN Sezione di Napoli[a]; Dipartimento di Scienze Fisiche,
Università di Napoli Federico II[b], I-80126 Napoli, Italy
[49]NIKHEF, National Institute for Nuclear Physics and High Energy Physics, NL-1009 DB Amsterdam, The Netherlands
[50]University of Notre Dame, Notre Dame, Indiana 46556, USA
[51]Ohio State University, Columbus, Ohio 43210, USA
[52]University of Oregon, Eugene, Oregon 97403, USA
[53]INFN Sezione di Padova[a]; Dipartimento di Fisica, Università di Padova[b], I-35131 Padova, Italy
[54]Laboratoire de Physique Nucléaire et de Hautes Energies,
IN2P3/CNRS, Université Pierre et Marie Curie-Paris6,
Université Denis Diderot-Paris7, F-75252 Paris, France
[55]INFN Sezione di Perugia[a]; Dipartimento di Fisica, Università di Perugia[b], I-06100 Perugia, Italy
[56]INFN Sezione di Pisa[a]; Dipartimento di Fisica,
Università di Pisa[b]; Scuola Normale Superiore di Pisa[c], I-56127 Pisa, Italy
[57]Princeton University, Princeton, New Jersey 08544, USA
[58]INFN Sezione di Roma[a]; Dipartimento di Fisica,
Università di Roma La Sapienza[b], I-00185 Roma, Italy
[59]Universität Rostock, D-18051 Rostock, Germany
[60]Rutherford Appleton Laboratory, Chilton, Didcot, Oxon, OX11 0QX, United Kingdom
[61]CEA, Irfu, SPP, Centre de Saclay, F-91191 Gif-sur-Yvette, France
[62]SLAC National Accelerator Laboratory, Stanford, California 94309 USA
[63]University of South Carolina, Columbia, South Carolina 29208, USA
[64]Southern Methodist University, Dallas, Texas 75275, USA
[65]Stanford University, Stanford, California 94305-4060, USA
[66]State University of New York, Albany, New York 12222, USA
[67]Tel Aviv University, School of Physics and Astronomy, Tel Aviv, 69978, Israel
[68]University of Tennessee, Knoxville, Tennessee 37996, USA
[69]University of Texas at Austin, Austin, Texas 78712, USA
[70]University of Texas at Dallas, Richardson, Texas 75083, USA
[71]INFN Sezione di Torino[a]; Dipartimento di Fisica Sperimentale, Università di Torino[b], I-10125 Torino, Italy
[72]INFN Sezione di Trieste[a]; Dipartimento di Fisica, Università di Trieste[b], I-34127 Trieste, Italy
[73]IFIC, Universitat de Valencia-CSIC, E-46071 Valencia, Spain
[74]University of Victoria, Victoria, British Columbia, Canada V8W 3P6
[75]Department of Physics, University of Warwick, Coventry CV4 7AL, United Kingdom
[76]University of Wisconsin, Madison, Wisconsin 53706, USA

(Dated: August 3, 2010)

We present a search for the decay $B^+ \to \tau^+\nu_\tau$ using 467.8×10^6 $B\overline{B}$ pairs collected at the $\Upsilon(4S)$ resonance with the *BABAR* detector at the SLAC PEP-II B-Factory. We select a sample of events with one completely reconstructed B^- in an hadronic decay mode ($B^- \to D^{(*)0}X^-$ and $B^- \to J/\psi\, X^-$). We examine the rest of the event to search for a $B^+ \to \tau^+\nu$ decay. We identify the τ^+ lepton in the following modes: $\tau^+ \to e^+\nu_e\overline{\nu}_\tau$, $\tau^+ \to \mu^+\nu_\mu\overline{\nu}_\tau$, $\tau^+ \to \pi^+\overline{\nu}_\tau$ and $\tau^+ \to \rho\overline{\nu}_\tau$. We find an excess of events with respect to expected background, which excludes the null signal hypothesis at the level of 3.3 σ and can be converted to a branching fraction central value of $\mathcal{B}(B^+ \to \tau^+\nu_\tau) = (1.80^{+0.57}_{-0.54}(\text{stat.}) \pm 0.26(\text{syst.})) \times 10^{-4}$.

INTRODUCTION

The study of the purely leptonic decay is of particular interest as a test of the Standard Model (SM) and a search for physics beyond the SM. It is sensitive to the product of the B meson decay constant f_B, and the absolute value of the Cabibbo-Kobayashi-Maskawa matrix element $|V_{ub}|$ [1]. In the SM the branching fraction is given by:

$$\mathcal{B}(B^+ \to \tau^+\nu) = f_B^2 |V_{ub}|^2 \frac{G_F^2 m_B m_\tau^2}{8\pi} \left[1 - \frac{m_\tau^2}{m_B^2}\right]^2 \tau_{B^+}, \quad (1)$$

where G_F is the Fermi constant, τ_{B^+} is the B^+ lifetime, and m_B and m_τ are the B^+ meson and τ lepton masses.

The process is sensitive to possible extensions of the SM. For instance, in two-Higgs doublet models [2] and in minimal supersymmetric extensions of the SM it can be mediated by a charged Higgs boson. A branching fraction measurement can therefore also be used to constrain the parameter space of extensions of the SM. In a previously published analysis, based on a tagging technique using hadronic B decays that is similar to that used in this paper and a smaller data set, the *BABAR* collaboration measured $\mathcal{B}(B^+ \to \tau^+\nu_\tau) = (1.8^{+0.9}_{-0.8}(\text{stat.}) \pm 0.4 \pm 0.2(\text{syst.})) \times 10^{-4}$ [3], and using tagging based on reconstruction of semileptonic B decays $\mathcal{B}(B^+ \to \tau^+\nu_\tau) = (1.7 \pm 0.8(\text{stat.}) \pm 0.2(\text{syst.})) \times 10^{-4}$ [4]. The Belle collaboration measured, with a similar tagging technique used in this analysis, the branching fraction to be $\mathcal{B}(B^+ \to \tau^+\nu_\tau) = (1.79^{+0.56}_{-0.49}(\text{stat.})^{+0.46}_{-0.51}(\text{syst.})) \times 10^{-4}$ [5], and using a tagging algorithm based on the reconstruction of semileptonic B decays $\mathcal{B}(B^+ \to \tau^+\nu_\tau) = (1.54^{+0.38}_{-0.37}(\text{stat.})^{+0.29}_{-0.31}(\text{syst.})) \times 10^{-4}$ [6].

THE *BABAR* DETECTOR AND DATASET

The data used in this analysis were collected with the *BABAR* detector at the PEP-II storage ring. The sample corresponds to an integrated luminosity of $426\,\text{fb}^{-1}$ at the $\Upsilon(4S)$ resonance (on-resonance) and $44.5\,\text{fb}^{-1}$ taken at 40 MeV below the $B\bar{B}$ production threshold (off-resonance), which is used to study background from $e^+e^- \to f\bar{f}$ ($f = u, d, s, c, \tau$) continuum events. The on-resonance sample contains $(467.8 \pm 5.1) \times 10^6$ $B\overline{B}$ decays. The detector is described in detail elsewhere [7]. Charged particle trajectories are measured in the tracking system composed of a five-layer silicon vertex detector and a 40-layer drift chamber (DCH), operating in a 1.5 T solenoidal magnetic field. A Cherenkov detector is used for charged π–K discrimination, a CsI calorimeter (EMC) for photon and electron identification, and the flux return of the solenoid, which consists of layers of iron interspersed with resistive plate chambers or limited streamer tubes, for muon and neutral hadron identification.

In order to estimate signal selection efficiencies and to study physics backgrounds, we use a Monte Carlo (MC) simulation based on `GEANT4` [8]. In MC simulated signal events one B^+ meson decays as $B^+ \to \tau^+\nu_\tau$ and the other decays in any final state. The $B\overline{B}$ and continuum MC samples are equivalent to approximatively three times and 1.5 times, respectively, the accumulated data sample. Beam-related background and detector noise are taken from data and overlaid on the simulated events.

SIGNAL SELECTION

We reconstruct an exclusive decay of one of the B mesons in the event (which we refer to as the tag B) and examine the rest of the event for the experimental signature of $B^+ \to \tau^+\nu_\tau$ (charged-conjugate modes are implied throughout the paper). We consider the most abundant τ decay modes $\tau^+ \to e^+\nu\bar{\nu}$, $\tau^+ \to \mu^+\nu\bar{\nu}$, $\tau^+ \to \pi^+\nu$, $\tau^+ \to \rho^+\nu$, totaling approximatively 70% of all τ decays. The signal region in data is kept blind until the end of the analysis chain when we extract the signal yield. We reconstruct the tag B candidate in the set of hadronic decays $B^- \to M^0 X^-$, where M^0 denotes a $D^{(*)0}$ or a J/ψ, and X^- denotes a system of hadrons with total charge -1 composed of $n_1\pi^\pm$, $n_2 K^\pm$, $n_3\pi^0$, $n_4 K^0_S$ where $n_1 + n_2 \leq 5$, $n_2 \leq 2$, n_3 and $n_4 \leq 2$. We reconstruct the D^0 as $D^0 \to K^-\pi^+, K^-\pi^+\pi^0, K^-\pi^+\pi^-\pi^+, K^0_S\pi^0, K^0_S\pi^+\pi^-, K^0_S\pi^+\pi^-\pi^0, K^+K^-, \pi^+\pi^-$. We reconstruct the D^{*0} meson as $D^{*0} \to D^0\pi^0, D^0\gamma$, and the J/ψ meson as $J/\psi \to e^+e^-, \mu^+\mu^-$. The kinematic consistency of the tag B candidates is checked with the beam energy-substituted mass $m_{\rm ES} = \sqrt{s/4 - p_B^2}$ and the energy difference $\Delta E = E_B - \sqrt{s}/2$, where $\sqrt{s}$ is the total energy in the $\Upsilon(4S)$ center of mass system and p_B and E_B denote respectively the momentum and the energy of the tag B candidate in the center of mass frame. The resolution on ΔE is measured to be $\sigma_{\Delta E} = 10 - 35$ MeV, depending on the decay mode; we require $|\Delta E| < 3\sigma_{\Delta E}$. Events with a candidate tag B arise from two possible classes with different $m_{\rm ES}$ distributions. Signal events with a correctly reconstructed tag B and the other B decaying as $B \to \tau\nu$, and background events from $\Upsilon(4S) \to B^+B^-$ with a correctly reconstructed tag

B are characterized by an $m_{\rm ES}$ distribution peaked at the B mass. The other class of events consists of continuum background, $e^+e^- \to q\overline{q}$ ($q = u, , s,)$ and $e^+e^- \to \tau^+\tau^-$, and combinatorial background, $\Upsilon(4S) \to B^0\overline{B}^0$ or B^+B^- in which the tag B is misreconstructed; this class of events has a broad $m_{\rm ES}$ distribution that can be modeled by means of a phenomenological threshold function (ARGUS function) [9].

If multiple tag B candidates are reconstructed we select that with the lowest value of $|\Delta E|$. The purity $\mathcal{P}$ of each reconstructed B decay mode is estimated as the ratio of the number of peaking events with $m_{ES} > 5.27\,\mathrm{GeV}$ to the total number of events in the same range. We consider only events with the tag B reconstructed in decay modes with $\mathcal{P} > 0.1$. The yield in data is determined by means of an extended unbinned maximum likelihood fit to the $m_{\rm ES}$ distribution, as shown in figure 1. We use as probability density function (PDF) for the combinatorial and continuum background an ARGUS function, while for the correctly reconstructed tag B component we use as PDF a Gaussian function with an exponential tail (Crystal Ball function) [10]. Combinatorial and continuum backgrounds in any discriminating variable are estimated from a sideband in $m_{\rm ES}$ ($5.209\,\mathrm{GeV} < m_{\rm ES} < 5.260\,\mathrm{GeV}$) and extrapolated into the signal region ($m_{\rm ES} > 5.270\,\mathrm{GeV}$) using the results of a fit to an ARGUS function. The peaking B^+B^- background is determined from B^+B^- MC, after subtraction of the combinatorial component to avoid double counting by means of a similar fit.

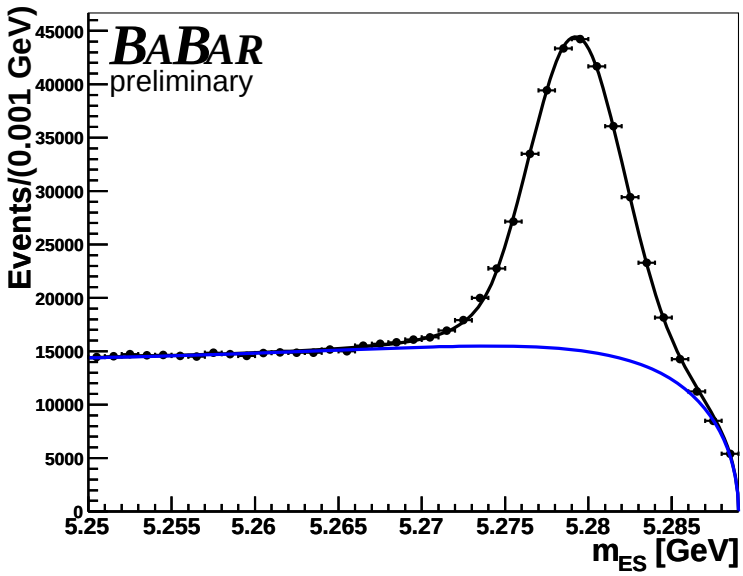

FIG. 1: Fit to the $m_{\rm ES}$ distribution in data. Dots are data, the blue curve represents the fitted combinatorial and continuum background.

After the reconstruction of the tag B, we apply a set of selection criteria on the rest of the event. We require the presence of only one well reconstructed charged track (signal track), with charge opposite to that of the tag B. The τ lepton is reconstructed in one of four decay modes: $\tau^+ \to e^+\nu\bar{\nu}$, $\tau^+ \to \mu^+\nu\bar{\nu}$, $\tau^+ \to \pi^+\nu$, $\tau^+ \to \rho^+\nu$. We separate the event sample in four categories using particle identification criteria applied to the signal track. The $\tau^+ \to \rho^+\nu$ sample is obtained by associating the signal track with a π^0 reconstructed from a pair of neutral clusters with invariant mass between 115 MeV/c^2 and 155 MeV/c^2. In order to remove the $e^+e^- \to \tau^+\tau^-$ background we impose τ mode dependent requirements, preserving 90% of the $B^+ \to \tau^+\nu_\tau$ signal, on the ratio between the 2^{nd} and the 0^{th} Fox-Wolfram moments (R2) [11] calculated using all the charged tracks and neutral clusters of the event.

In order to reject the continuum and combinatorial background we use discriminating variables constructed from the kinematics of the tag B candidate. The first variable is the momentum in the CM frame (p^*_M) of the $D^{(*)0}$ or J/ψ candidate reconstructed from the decay products of the tag B. The second variable is the absolute value of the thrust [12] ($|\vec{T_B}|$) of the tag B. The third variable is the cosine of the angle between the thrust of the tag B and the thrust of the rest of the event ($\cos\theta_{TB}$). We combine p^*_M, $|\vec{T_B}|$ and $\cos\theta_{TB}$ in a likelihood ratio $L_C = L_S(p^*_M, |\vec{T_B}|, \cos\theta_{TB})/(L_S(p^*_M, |\vec{T_B}|, \cos\theta_{TB}) + L_B(p^*_M, |\vec{T_B}|, \cos\theta_{TB}))$, where the signal ($S$) and background ($B$) likelihoods are obtained from the products of the PDFs of the three discriminating variables: $L_S(p^*_M, |\vec{T_B}|, \cos\theta_{TB}) = P_S(p^*_M)P_S(|\vec{T_B}|)P_S(\cos\theta_{TB})$ and $L_B(p^*_M, |\vec{T_B}|, \cos\theta_{TB}) = P_B(p^*_M)P_B(|\vec{T_B}|)P_B(\cos\theta_{TB})$.

The PDFs for the signal modes are obtained from the signal MC, whereas the PDFs for backgrounds are obtained from the $m_{\rm ES}$ sideband in data.

In order to further reject the background from correctly reconstructed tag B events, we impose a requirement on center of mass momentum of the signal track for the $\tau^+ \to e^+\nu\bar{\nu}$, $\tau^+ \to \mu^+\nu\bar{\nu}$ and $\tau^+ \to \pi^+\nu$ modes. For the $\tau^+ \to \rho^+\nu$ mode we combine in a likelihood ratio (L_P) the following variables: the invariant mass of the signal track and the π^0, the total momentum in the CM frame of the pair $|\vec{p}^{\,*}_\rho|$, the momentum in the CM frame of the π^0, and the missing mass of the event. The PDFs used in the likelihood ratio for the signal and background are determined from signal and B^+B^- MC, respectively.

The most discriminating variable is $E_{\rm extra}$, defined as the sum of the energies of the neutral clusters not associated with the tag B or with the signal π^0 from the $\tau^+ \to \rho^+\nu$ mode, and passing a minimum energy requirement (60 MeV). Signal events tend to peak at low $E_{\rm extra}$, background events, which contain additional sources of neutral clusters, tend to be distributed at higher values.

We optimize the selection requirements, including those on the purity $\mathcal{P}$ of the tag B and the minimum energy of the neutral clusters, aiming at the lowest expected uncertainty in the branching fraction fit. In order to estimate the uncertainty, which includes the statistical and the largest systematic uncertainties, we run 1000 toy experiments extracted from the background and signal expected shapes for a set of possible selection requirements, assuming a branching fraction of 1.4×10^{-4}[13].

The signal selection requirements are summarized in table I. The $E_{\rm extra}$ distribution with all the selection requirements applied is shown in figure 2.

Variable	$\tau^+ \to e^+\nu\bar{\nu}$	$\tau^+ \to \mu^+\nu\bar{\nu}$	$\tau^+ \to \pi^+\nu$	$\tau^+ \to \rho^+\nu$
purity		$> 10\%$		
cluster energy (MeV)		60		
R2	< 0.57	< 0.56	< 0.56	< 0.51
L_C	> 0.2	> 0	> 0.3	> 0.45
p^*_{trk}(GeV/c)	< 2.1	< 2	> 1.4	
L_P				> 0.8

TABLE I: Optimized signal selection criteria for each τ mode.

BRANCHING FRACTION MEASUREMENT PROCEDURE AND RESULTS

We use an extended unbinned maximum likelihood fit to extract the $B^+ \to \tau^+\nu$ branching fraction. The likelihood function for the N_k candidates reconstructed in one of the four τ decay modes k is

$$\mathcal{L}_k = e^{-(n_{s,k}+n_{b,k})} \prod_{i=1}^{N_k} \left\{ n_{s,k}\mathcal{P}^s_k(E_{i,k}) + n_{b,k}\mathcal{P}^b_k(E_{i,k}) \right\} \tag{2}$$

where $n_{s,k}$ is the signal yield, $n_{b,k}$ is the background yield, $E_{i,k}$ is the $E_{\rm extra}$ value of the i^{th} event, $\mathcal{P}^s_k$ is the probability density function of signal events, and $\mathcal{P}^b_k$ is the probability density function of background events. The background yields in each decay mode are permitted to float independently of each other in the fit, while the signal yields are constrained to a single branching ratio via the relation:

$$n_{s,k} = N_{B\overline{B}} \times \epsilon_k \times \mathcal{B} \tag{3}$$

where $N_{B\overline{B}} = (4.678 \pm 0.051) \times 10^8$ is the number of $B\overline{B}$ pairs in the data sample, ϵ_k is the τ decay mode dependent reconstruction efficiency, and $\mathcal{B}$ is the $B^+ \to \tau^+\nu$ branching fraction. The parameters $N_{B\overline{B}}$ and ϵ_k are fixed in the fit while $\mathcal{B}$ is left floating. The reconstruction efficiencies ϵ_k, which include the τ branching fractions, are obtained from MC simulation of the signal. Since the tag B reconstruction efficiency is included in ϵ_k and is estimated from the signal MC, we apply a correction factor $R_{\rm data/MC} = 0.926 \pm 0.010$ to take into account data/MC differences, taking the ratio of the peaking component of the $m_{\rm ES}$ distribution of the hadronic tag B in data and in MC simulation events.

We use histograms with a bin width of 60 MeV to represent the PDFs $\mathcal{P}^s_k$ and $\mathcal{P}^b_k$ for signal and background, respectively. The signal PDF is obtained from a high statistics signal MC simulation sample, corrected for data/MC

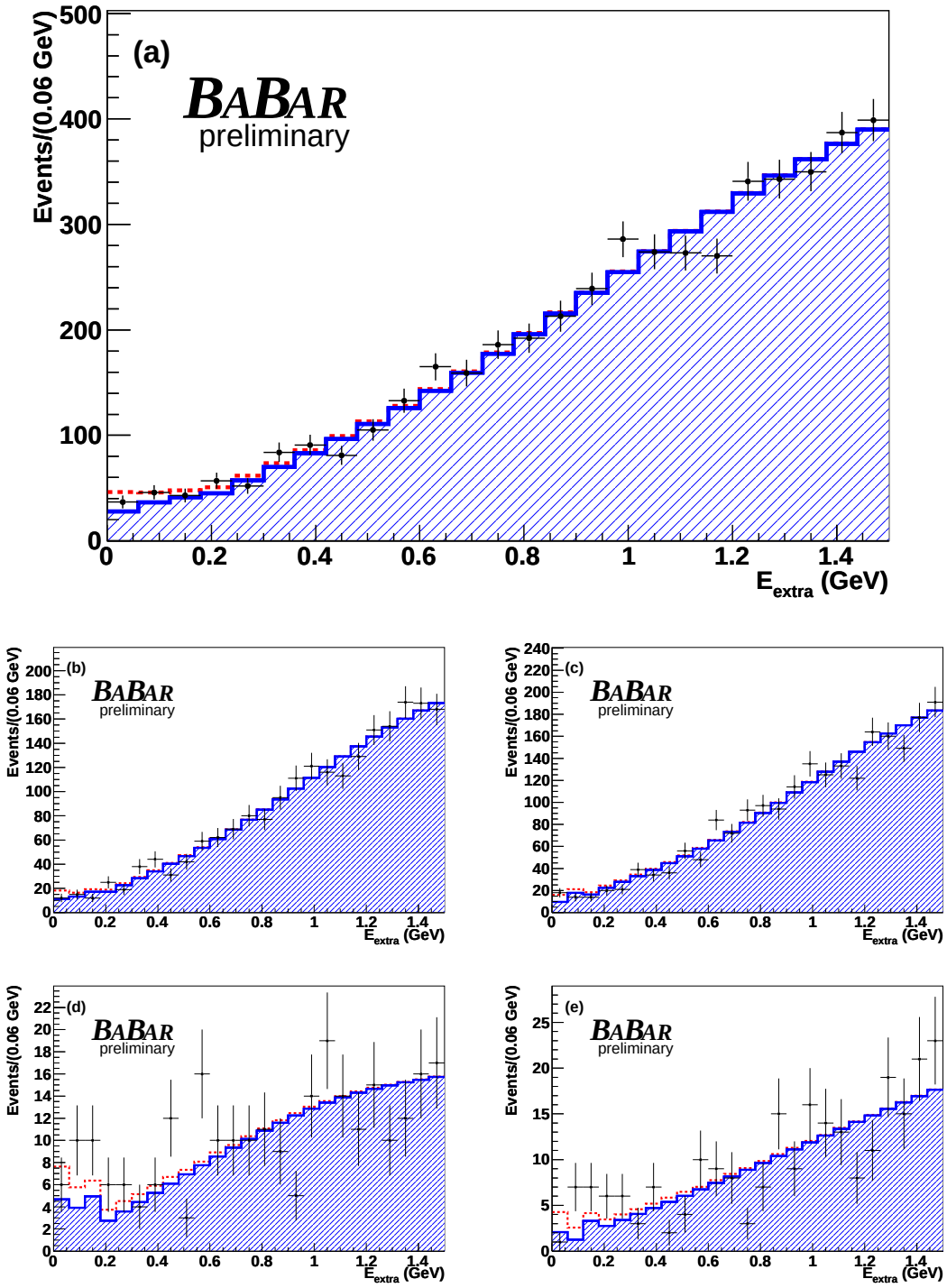

FIG. 2: $E_{\rm extra}$ distribution in data (dots with error bars) with all selection requirements applied and fit results overlaid. The hatched histogram is the background, the red dashed component is the signal. Plot *(a)* shows all τ decay modes fitted simultaneously. Lower plots show the projection of the simultaneous fit result on the four analyzed τ decay modes: *(b)* $\tau^+ \to e^+\nu\bar{\nu}$, *(c)* $\tau^+ \to \mu^+\nu\bar{\nu}$, *(d)* $\tau^+ \to \pi^+\nu$, *(e)* $\tau^+ \to \rho^+\nu$.

disagreement. Since a data sample of suitable statistics with exactly the same final states as our signal channels is not available, we use a sample of fully reconstructed events where in addition to the reconstructed tag B, a second B is

Decay Mode	$\epsilon \times 10^{-4}$	Branching Fraction ($\times 10^{-4}$)	Significance σ
$\tau^+ \to e^+\nu\bar{\nu}$	2.73	$0.39^{+0.89}_{-0.79}$	0.5
$\tau^+ \to \mu^+\nu\bar{\nu}$	2.92	$1.23^{+0.89}_{-0.80}$	1.6
$\tau^+ \to \pi^+\nu$	1.55	$4.0^{+1.5}_{-1.3}$	3.3
$\tau^+ \to \rho^+\nu$	0.85	$4.3^{+2.2}_{-1.9}$	2.6
combined	8.05	$1.80^{+0.57}_{-0.54}$	3.6

TABLE II: Reconstruction efficiency ϵ, measured branching fractions and statistical significance obtained from the fit with all the modes separately and constrained to the same branching fraction. The τ decay mode branching fractions are included in the efficiencies.

reconstructed in an hadronic or a semileptonic decay mode, using charged tracks and neutral clusters not assigned to the tag B. In order to estimate the correction to the signal PDF, we compare the distribution of $E_{\rm extra}$ in this double tags sample from experimental data and MC simulation. The distributions are normalized to the same area and the comparison is shown in figure 3. We extract the correction function taking the ratio of the two distributions and fitting it with a second order polynomial.

We take the PDF of the combinatorial background from the $m_{\rm ES}$ sideband. The contribution of this component in the signal region is obtained by fitting the $m_{\rm ES}$ distribution after the selection has been applied. The shape of the peaking background is taken from B^+B^- MC in the signal region, after the intrinsic combinatoric background has been subtracted by a fit to $m_{\rm ES}$, to avoid double counting. The two background components are added together in a single background PDF. We finally apply a smoothing procedure on the total background shape, excluding the first bins. We estimate the branching fraction minimizing $-2\ln\mathcal{L}$, where $\mathcal{L} = \Pi_{k=1}^{4}\mathcal{L}_k$, and $\mathcal{L}_k$ is defined in equation 2.The projections of the fit results are shown in figure 2. We observe a significant excess of events with respect to the expected backgrounds and measure a branching fraction $\mathcal{B}(B^+ \to \tau^+\nu_\tau) = (1.80^{+0.57}_{-0.54}) \times 10^{-4}$, where the uncertainty is statistical. We evaluate the significance of the observed signal, including only statistical uncertainty, as $S = \sqrt{2\ln(\mathcal{L}_{s+b}/\mathcal{L}_b)}$, where $\mathcal{L}_{s+b}$ and $\mathcal{L}_s$ denotes the obtained maximum likelihood value and the likelihood value assuming background only. We find $S = 3.6\sigma$. Table II summarizes the results from the fit.

SYSTEMATICS

The dominant source of systematic uncertainty is the background PDF, due the finite statistics of the B^+B^- MC simulated sample, used to estimate the B^+B^- background PDF, and of the $m_{\rm ES}$ data sideband, used to estimate the combinatorial and continuum backgrounds. In order to estimate the systematic uncertainty we repeat the fit of the branching fraction with 1000 variations of the background PDF, varying each bin within the statistical error, and assign 12% as systematic uncertainty.

The systematic uncertainty due to the signal $E_{\rm extra}$ distribution correction function obtained from data/MC comparisons using control samples is obtained by varying the parameters of the second order polynomial within their uncertainty and repeating the fit to the $B^+ \to \tau^+\nu_\tau$ branching fraction. We observe a 1.7% variation that we take as the systematic uncertainty on the signal shape.

Uncertainty in the differences between data and MC in the tracking and neutral reconstruction efficiencies reflects in the uncertainty in the central value of the branching fraction. The difference of the tracking efficiency is estimated with a control sample of high momentum tracks from $e^+e^- \to \tau^+\tau^-$ events to be 0.5% per track. Since there is only one signal track candidate in all four τ decay modes in the $B^+ \to \tau^+\nu_\tau$ signal, we use this value as the uncertainty due to tracking efficiency. We accept events with one extra low p_T charged track. Comparing the multiplicity of low p_T charged tracks from the double tags sample in data and in MC, we estimate the systematic uncertainty to be 1.3%. Adding in quadrature the two uncertainties we estimate the the systematic error to be 1.4%.

Other systematic uncertainties on the efficiency stem from the finite signal MC statistics (0.8%), the uncertainty in the tag B efficiency correction (5.0%), the electron identification (2.6%), and muon identification (4.7%). The systematic uncertainties are summarized in Table III. The total systematic uncertainty is obtained by combining all sources in quadrature.

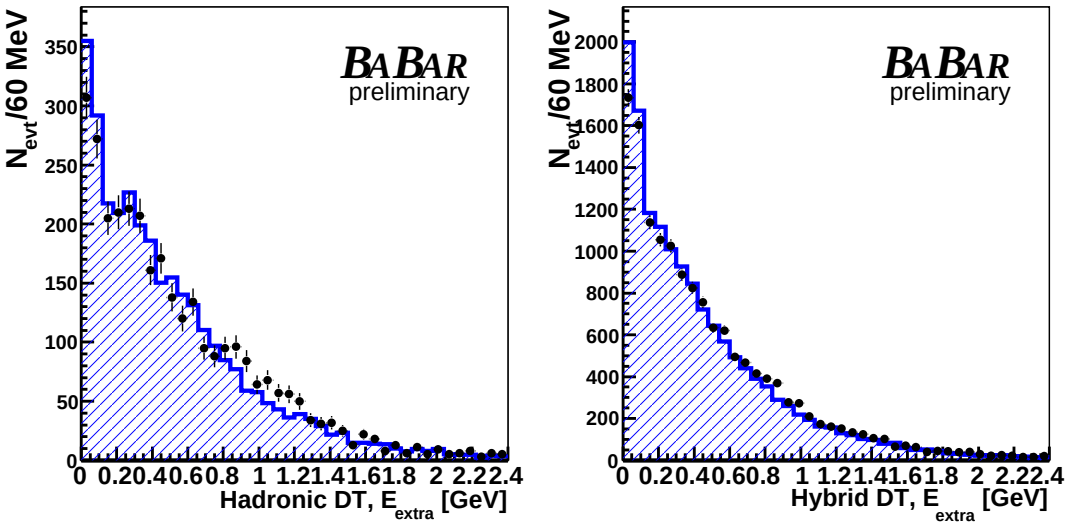

FIG. 3: $E_{\rm extra}$ distribution for double tags. The second B is reconstructed in hadronic decays (left plot) or semileptonic decays (right plot). Points are data, histograms are MC simulation.

Source of systematics	BF uncertainty (%)
B counting	0.5
Tag B efficiency	5.0
Background PDF	12
Signal PDF	1.7
MC statistics	0.8
Electron identification	2.6
Muon identification	4.7
Kaon identification	0.4
Tracking	1.4
Total	14

TABLE III: Contributions to systematic uncertainty on the branching fraction.

CONCLUSIONS

In summary, we have measured the branching fraction of the decay $B^+ \to \tau^+\nu_\tau$ using a tagging algorithm based on the reconstruction of hadronic B decays using a data sample containg 467.8×10^6 $B\overline{B}$ pairs collected with the *BABAR* detector at the PEP-II B-Factory. We measure the branching fraction to be $\mathcal{B}(B^+ \to \tau^+\nu_\tau) = (1.80^{+0.57}_{-0.54}(\text{stat.}) \pm 0.26(\text{syst.})) \times 10^{-4}$, excluding the null hypothesis at the level of 3.6 standard deviations using statistical uncertainties only, and at the level of 3.3 standard deviations including the systematic uncertainties. This result supersedes our previous result using the same technique [3]. Combining this result with the other *BABAR* measurement of $\mathcal{B}(B^+ \to \tau^+\nu_\tau)$ derived from a statistically independent sample [4], we obtain a single *BABAR* result $\mathcal{B}(B^+ \to \tau^+\nu_\tau) = (1.76 \pm 0.49) \times 10^{-4}$, where the uncertainty includes both statistical and systematic uncertainties.

ACKNOWLEDGEMENTS

We are grateful for the extraordinary contributions of our PEP-II colleagues in achieving the excellent luminosity and machine conditions that have made this work possible. The success of this project also relies critically on the expertise and dedication of the computing organizations that support *BABAR*. The collaborating institutions wish to thank SLAC for its support and the kind hospitality extended to them. This work is supported by the US Department of Energy and National Science Foundation, the Natural Sciences and Engineering Research Council (Canada),

the Commissariat à l'Energie Atomique and Institut National de Physique Nucléaire et de Physique des Particules (France), the Bundesministerium für Bildung und Forschung and Deutsche Forschungsgemeinschaft (Germany), the Istituto Nazionale di Fisica Nucleare (Italy), the Foundation for Fundamental Research on Matter (The Netherlands), the Research Council of Norway, the Ministry of Education and Science of the Russian Federation, Ministerio de Ciencia e Innovación (Spain), and the Science and Technology Facilities Council (United Kingdom). Individuals have received support from the Marie-Curie IEF program (European Union), the A. P. Sloan Foundation (USA) and the Binational Science Foundation (USA-Israel).

* Now at Temple University, Philadelphia, Pennsylvania 19122, USA
† Also with Università di Perugia, Dipartimento di Fisica, Perugia, Italy
‡ Also with Università di Roma La Sapienza, I-00185 Roma, Italy
§ Now at University of South Alabama, Mobile, Alabama 36688, USA
¶ Also with Università di Sassari, Sassari, Italy

[1] N. Cabibbo, Phys. Rev. Lett. **8**, 214 (1964); M. Kobayashi and T. Maskawa, Prog. Theor. Phys. **49**, 652 (1973).
[2] W. S. Hou, Phys. Rev. D **48**, 2342 (1993).
[3] B. Aubert *et al.* (*BABAR* Collaboration), Phys. Rev. D **77**, 011107(R) (2008).
[4] B. Aubert *et al.* (*BABAR* Collaboration), Phys. Rev. D **81**,051101(R) (2010).
[5] K. Ikado *et al.* (Belle Collaboration), Phys. Rev. Lett. **97**, 261802 (2006).
[6] K. Hara, T. Iijima, *et al.* (Belle Collaboration), arXiv:1006.4201[hep-ex].
[7] B. Aubert *et al.* (*BABAR* Collaboration), Nucl. Instrum. Methods Phys. Res., Sect. A **479**, 1 (2002); W. Menges, IEEE Nucl. Sci. Symp. Conf. Rec. **5**, 1470 (2006).
[8] S. Agostinelli *et al.* (GEANT4 Collaboration) Nucl. Instrum. Methods Phys. Res., Sect. A **506**, 250 (2003).
[9] H. Albrecht *et al.* (ARGUS Collaboration) Phys. Lett. B **185**, 218 (1987).
[10] M. J. Oreglia, Report no. SLAC-236, 1980; J. E. Gaiser, Report No. SLAC-255, 1982; T. Skwarnicki, Report No. DESY F31-86-02, 1986.
[11] G. C. Fox and S. Wolfram, Nucl. Phys. B **149** (1979) 413.
[12] E. Farhi, Phys. Rev. Lett. **39**, 1587 (1977).
[13] C. Amsler *et al.* (Particle Data Group),Phys. Lett. B **667**, 1 (2008) and 2009 partial update for 2010 edition (URL: http://pdg.lbl.gov).